PACS numbers: 42.55.Rz; 42.25.Lc
DOI: 10.1070/QE2009v039n10ABEH014062

Thermally induced distortions in neodymium glass rod amplifiers*

A.A. Kuzmin, G.A. Luchinin, A.K. Poteomkin, A.A. Soloviev, E.A. Khazanov, A.A. Shaykin

***Abstract*. The depolarisation dynamics in a neodymium glass rod laser amplifier is experimentally studied. A method for determining the temperature distribution and the thermally induced phase distortions from the known transverse depolarisation degree distribution is proposed. The experimental results obtained by this method perfectly coincide with the theoretical results even at a strong radial inhomogeneity of the heat release.**

Keywords: *neodymium glass, induced birefringence, thermal lens, thermally induced depolarisation.*

1. Introduction

In recent years, increasing interest has been focused on neodymium glass lasers emitting nanosecond pulses. These lasers are widely used in experiments on laser thermonuclear fusion and in other fundamental and applied studies. They are also indispensable for developing femtosecond laser systems with a petawatt power. Depending on the amplifying medium used, all the existing and designed petawatt lasers can be divided into three types: neodymium glass lasers [1–5], Ti : sapphire lasers [6–9], and DKDP parametric amplifiers [10]. In all the cases, the energy is first stored in a nanosecond pulse of a neodymium glass laser. For the lasers of the first type, this pulse is compressed, while in the lasers of the second and third types the energy of this pulse is converted into the second harmonic, which is used for pumping chirped-pulse amplifiers.

The maximum pulse repetition rate in these lasers varies, depending on the active element size, from one pulse per ten seconds to one pulse per day, which is much smaller than in systems based on crystals or ceramics. The pulse repetition rate is limited by thermal effects in the neodymium glass caused by a low thermal conductivity and a large aperture of glass amplifiers.

The fundamental limit is the breakdown of glass as the thermally induced stresses exceed a critical value. However, in practice, lasers are used at considerably lower repetition rates. This is explained by the appearance and accumulation of the beam depolarisation and by the formation of a strong aberrated thermal lens. These effects considerably deteriorate the laser beam quality.

In this paper, we study the thermally-induced depolarisation and the thermal lens in a cylindrical neodymium phosphate glass active element (AE). It is shown that, by measuring the depolarisation, one can determine the temperature distribution and the thermally induced phase at a random axially symmetric temperature distribution. The possibilities of increasing the pulse repetition rate are analysed.

2. Relation between the thermal lens and depolarisation in cylindrical active elements

Heating of a laser AE by pump lamp radiation forms a gradient in temperature T and, hence, deforms the element. This causes the isotropic change in the dielectric constant tensor ε (due to the temperature dependence of the refractive index)

$$\Delta\varepsilon_n = 2\beta n T, \tag{1}$$

as well as the anisotropic change in ε_{ij} (due to the photoelastic effect) [11]

$$\Delta\varepsilon_{ij}^{-1} = p_{ijkl}U_{kl}, \tag{2}$$

where $\beta = \mathrm{d}n/\mathrm{d}T$; n is the unperturbed refractive index; U_{kl} is the deformation tensor; and p_{ijkl} is the photoelasticity tensor. For an infinitely long cylinder in which T depends neither on z nor on φ (r, φ, z are the cylindrical coordinates), i.e., in the case of a radial deformation, there are only two nonzero deformation tensor components [12]:

$$U_{rr} = \frac{\alpha(1+\nu)}{1-\nu}\left[T(t,r) - \frac{1}{r^2}\int_0^r T(t,r)r\mathrm{d}r + \frac{1-2\nu}{R^2}\int_0^R T(t,r)r\mathrm{d}r\right], \tag{3}$$

$$U_{\varphi\varphi} = \frac{\alpha(1+\nu)}{1-\nu}\left[\frac{1}{r^2}\int_0^r T(t,r)r\mathrm{d}r + \frac{1-2\nu}{R^2}\int_0^R T(t,r)r\mathrm{d}r\right],$$

where α is the linear thermal expansion coefficient; ν is the Poisson ratio; and R is the AE radius.

* Reported at the Conference 'Laser Optics 2008', St. Petersburg, Russia.

A.A. Kuzmin, G.A. Luchinin, A.K. Poteomkin, A.A. Soloviev, E.A. Khazanov, A.A. Shaykin Institute of Applied Physics, Russian Academy of Sciences, ul. Ul'yanova 46, 603950 Nizhnii Novgorod, Russia; e-mail: khazanov@appl.sci-nnov.ru

Received 28 January 2009
Kvantovaya Elektronika **39** (10) 895–900 (2009)
Translated by M.N. Basieva

Due to the given symmetry of the deformation tensor, radiation propagating inside the AE can be expanded in eigenmodes polarised in the radial and tangential directions. The thermally induced changes in the refractive indices of these modes can be written in the form

$$n_{r(\varphi)} = \beta\Delta T + \frac{\Delta\varepsilon_{rr(\varphi\varphi)}}{2n}. \tag{4}$$

The birefringence leads to a depolarisation, i.e. in the case of a linearly polarised wave incident on the AE, the output wave contains an orthogonally polarised component with an intensity I_d, whose ratio to the total radiation intensity I_0 determines the depolarisation degree $\Gamma = I_d/I_0$. Using (2) and (4), we can derive

$$\Gamma(r,\varphi) = \sin^2(2\varphi)\sin^2\frac{\pi L n^3(p_{12}-p_{11})}{2\lambda}\left(U_{rr}-U_{\varphi\varphi}\right)$$

$$\equiv \sin^2(2\varphi)\Gamma(r), \tag{5}$$

where L is the AE length; λ is the laser radiation wavelength; p_{11} and p_{12} are the photoelasticity tensor components in the Nye two-index notation [13]. An isotropic medium is completely characterised by these two components. In practice, it is convenient to consider the aperture-integrated depolarisation degree $\gamma = P_d/P_0$, i.e. the ratio of the depolarised component power P_d to the total radiation power P_0.

Assuming that the AE is instantly heated by a pump lamp flash and that the boundary condition of the convective heat exchange with the environmental medium at $r = R$ is $\kappa \mathrm{d}T/\mathrm{d}r = -\alpha_c\Delta T$ ($\varkappa$ is the thermal conductivity coefficient, α_c is the convective heat exchange coefficient, and ΔT is the difference between the temperature at the AE surface and the temperature of the surrounding air), we can solve the equation for the thermal conductivity in the AE in the form of the series [14]

$$\Delta T(t,r) = \sum_{n=1}^{\infty} C_n \exp\left(-\frac{t}{\tau_n}\right) J_0(q_n r), \tag{6}$$

where ΔT is measured from the surrounding air temperature; $\tau_n = c_T\rho/(\kappa q_n^2)$ is the decay time of the nth term of the series; c_T and ρ are the specific heat and density of the AE, respectively; and q_n are the solutions of the equation

$$\frac{qJ_1(qR)}{J_0(qR)} = \frac{\alpha_c}{\kappa} \tag{7}$$

($J_{0,1}$ are the zero- and first-order Bessel functions of the first kind). The coefficients C_n are determined by the initial temperature distribution in the AE and are proportional to the energy absorbed in the rod. Solution (6) is valid if the temperature does not depend on z, i.e. for a long cylinder (whose length considerably exceeds its diameter) and a homogeneous distribution of temperature along z at the initial instant. The experiments described below well satisfy these conditions.

Comparing (3) and (5) and introducing the parameter $Q = \frac{1}{4}\alpha n^3[(1+\nu)/(1-\nu)](p_{11}-p_{12})$, we find

$$kLQ[\Delta T(r) - \Delta T(0)] = \mathrm{Arcsin}\sqrt{\Gamma(r)} + 2\int_0^r \frac{\mathrm{Arcsin}\sqrt{\Gamma(r)}}{r}\,\mathrm{d}r, \tag{8}$$

where $k = 2\pi/\lambda$; $\mathrm{Arcsin}\sqrt{\Gamma(r)} = (-1)^{m+n-1}\arcsin\sqrt{\Gamma(r)} + \pi m$; and m and n are the numbers of points r_i and r_j in the range $[0, r]$ such that $\Gamma(r_i) = 1$ and $\Gamma(r_j) = 0$.

One can see from (8) that, knowing the depolarisation degree distribution $\Gamma(r)$ at a particular time instant, it is possible to calculate the temperature distribution $\Delta T(r)$ with an accuracy to the constant $\Delta T(r=0)$ at this instant and, according to (6), at all following instants. Knowing $\Delta T(r)$, one can calculate by (4) the thermal lens parameters, i.e. the thermally induced phase increments of eigenwaves in the AE $\Delta\psi_{r,\varphi} = kL\Delta n_{re,\varphi}$ by the expression

$$\Delta\psi_{r,\varphi} = 2\frac{P}{Q}\int_0^r \frac{\mathrm{Arcsin}\sqrt{\Gamma(\mathrm{r})}}{r}\,\mathrm{d}r + \left(\frac{P}{Q}\pm 1\right)\mathrm{Arcsin}\sqrt{\Gamma(\mathrm{r})}, \tag{9}$$

where $P = \beta - Q(p_{12}+p_{11})/(p_{12}-p_{11})$.

Thus, having measured the depolarisation degree $\Gamma(r)$, we can, with an accuracy to a constant, determine the temperature distribution $\Delta T(r)$ and the thermally induced phase for the waves of both polarisations. From the experimental viewpoint, it is much simpler to measure depolarisation than temperature or phase.

3. Experimental study of the depolarisation dynamics in neodymium glass rods

The depolarisation degree dynamics in an isotropic AE was experimentally studied by the example of a neodymium-doped phosphate glass rod 25 cm long and 15 mm in diameter. The concentration of neodymium ions was 1.5×10^{20} cm^{-3}. The AE was placed in a four-lamp pump cavity with a mirror reflector; the small-signal gain with the used pump energy storage system was about 60. We studied the thermooptical effects when the AE was cooled naturally or by air flow. The pump pulses were either single (spaced by times that considerably exceeded the temperature relaxation time) or successive, which simulated a real laser operation. Most attention was paid to the depolarisation appeared in the AE, because its effect on the laser beam quality was most pronounced. As was shown above, knowing the depolarisation, one can calculate both the temperature and the thermal lens parameters.

Figure 1 shows the distributions of the depolarisation degree Γ over the AE aperture 15 mm in diameter at different instants after a single pump pulse when the AE was cooled by air flow. During the first seconds after pumping, the maximum depolarisation degree at the beam edge is close to unity. Then, the region with a pronounced depolarisation moves inside the AE, and, after ten seconds from the pump pulse, the depolarisation begins to decrease. We do not show distributions for times exceeding one minute because, beginning from this time, the topology does not change and only the depolarisation amplitude decreases. In the case of natural cooling of the AE (without air flow), the distributions were similar to Fig. 1 except for the last frame, where the corresponding values were much smaller.

Figure 2 presents the time dependences of the aperture-integrated depolarisation degree after a single pump pulse

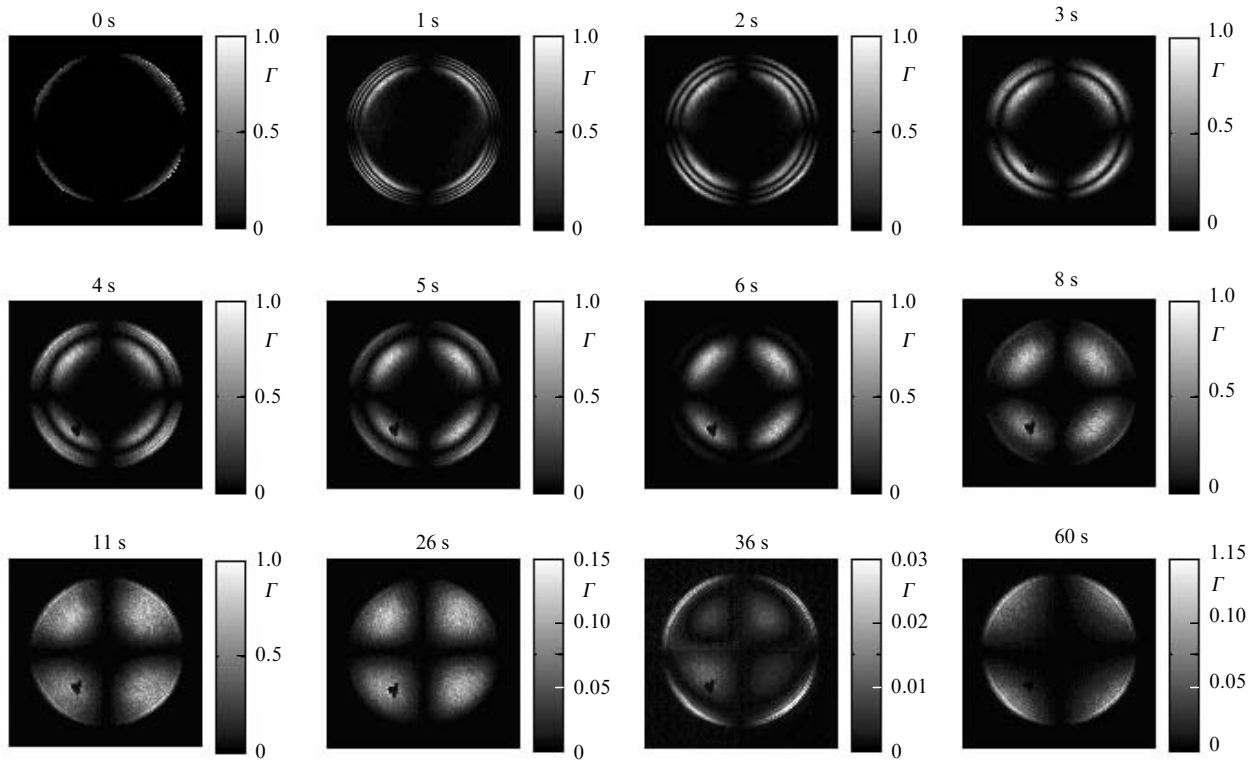

Figure 1. Distributions of the depolarisation degree Γ over the cross section of an AE 15 mm in diameter at different time instants after the pump pulse; the AE was cooled by air flow.

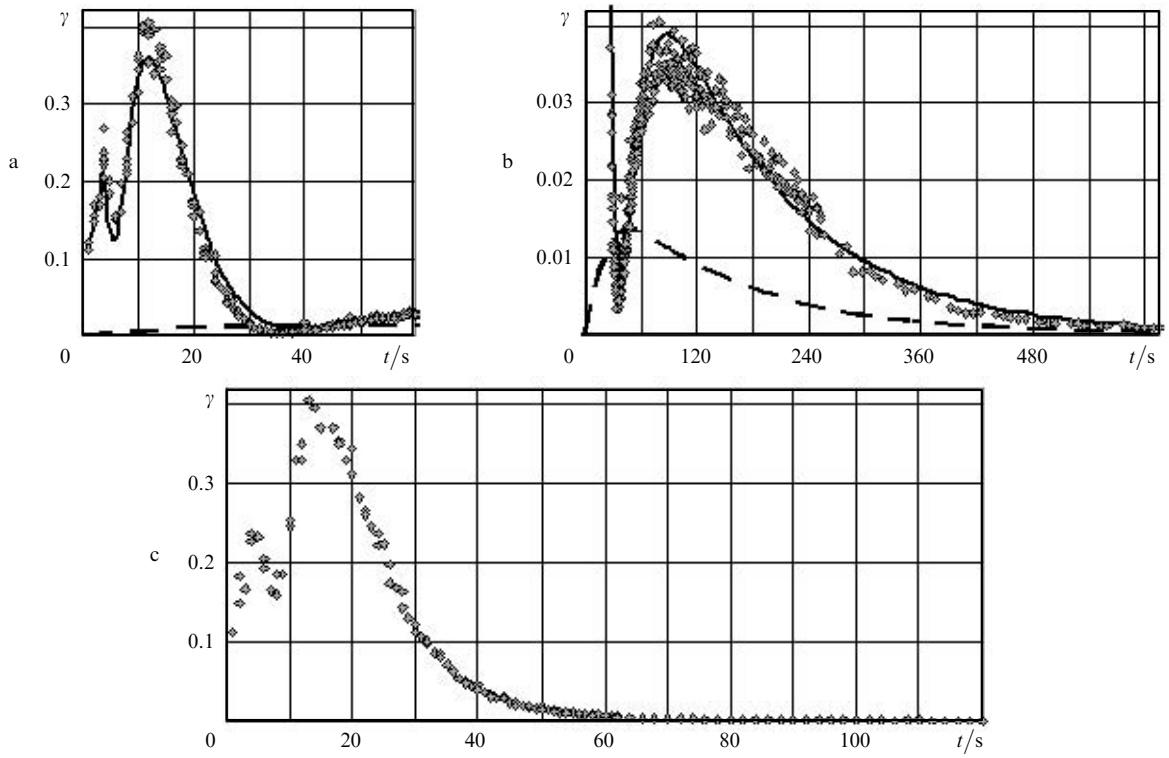

Figure 2. Dynamics of the integral depolarisation degree in an AE 15 mm in diameter after a single pump pulse in the case of forced-air (a, b) and natural (c) cooling. The solid curves show the theoretical dependences and the dashed curves correspond to the dependences plotted in the assumption of homogeneous heating of the AE. Figures a and b have different axis scales.

for natural cooling and for additional cooling of the AE by air flow. Figure 3 shows similar dependences for a train of pump pulses with a period of 5 min. This regime simulates a real laser operation.

4. Discussion of experimental results

Immediately after a pump pulse, the region with the maximum depolarisation lies very close to the lateral

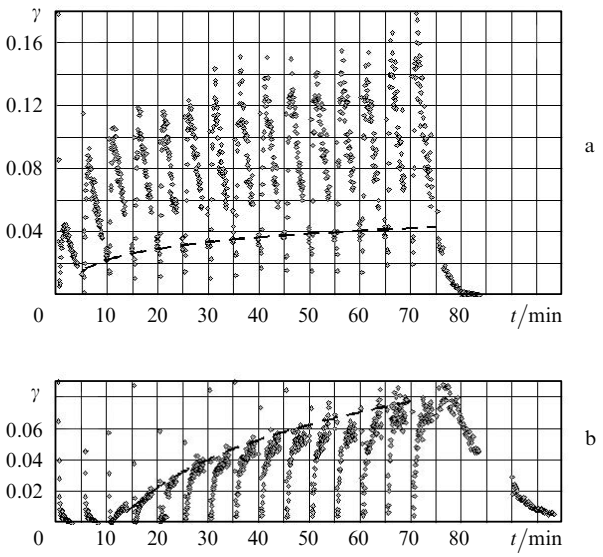

Figure 3. Dynamics of the integral depolarisation degree in trains of pump pulses with a period of 5 min for forced-air (a) and natural (b) cooling of the AE. The points corresponding to the first seconds after each pump pulse cannot be seen because they lie beyond the range of the y axis. The dashed curves connect the points corresponding to the depolarisation at the instants prior to the pump pulses.

surface of the AE and extends to its centre for the first seconds (see Fig. 1), while the time dependence of the integral depolarisation is nonmonotonic (Fig. 2). These two circumstances allow us to assume that a large portion of the thermal energy is absorbed in the near-surface region. As a result, for the first seconds after pumping, the high temperature gradient near the AE surface creates a large phase incursion in the edge beams. To calculate the temperature distribution and the phase incursion by expressions (8), (9), we used the experimental distribution $\Gamma(r)$ measured one second after the pump pulse (Fig. 1). The results are shown in Fig. 4. Expression (8) allows us to find $\Delta T(r)$ with an accuracy to the constant $\Delta T(0)$. This constant was determined using the time dependence of the integral depolarisation γ for a single pulse (Fig. 2). We calculated the constant of heat exchange with surrounding air ($\alpha_c = 35$ W m^{-2}K^{-1}) from the dependence $\gamma(t)$ at large times (Fig. 2b) and determined the temperature $\Delta T(0)$ at the AE centre by the best fit of the experimental points and the theoretical curve (see Fig. 2a). The resulting dependence is shown in Fig. 4a. Using this dependence as the initial temperature distribution, we calculated the further dynamics of temperature by expressions (6), (7) and the dynamics of depolarisation Γ by expressions (3), (5). The found distributions $\Gamma(r, \varphi)$ at all instants completely coincide with the experimental data given in Fig. 1.

The strong heating of the peripheral region (Fig. 4a) can be caused by several reasons: a too high doping of the AE, and, hence, a high absorption of pump radiation in the near-surface layer; the absorption of neodymium ions in the short-wavelength region of the pump lamp spectrum (for which the quantum defect is rather high); and the absorption of the pump lamp UV radiation by phosphate glass.

To eliminate the first reason, we measured a series of small-signal gains, which unambiguously determine the energy stored in the AE. The results are shown in Fig. 5.

From Fig. 5 one can see that the transverse gain distribution at small pump energies has a square shape with vertexes near the lamps (Fig. 5a); with increasing the pump energy, this distribution ceases to depend on the polar angle (Fig. 5b). With a further increase in the pump energy, the azimuthal inversion homogeneity is retained until strong thermooptical effects appear. The quite homogeneous gain distribution over the pump cavity cross section indicates that the dopant concentration is chosen correctly. Some decrease in the gain in the peripheral region can be explained by the existence of whispering gallery modes. To reduce this effect, it is necessary to use immersion.

Returning to Fig. 4a, we can see that, after a single pump pulse, the AE surface temperature increases by about 30 K, while the temperature of the central AE region increases by approximately 4 K. Because of this, due to a relatively high thermal conductivity of the AE, the heat flow to the environment is small compared to the flow directed inside the AE. Therefore, during the first seconds after the pump pulse, the depolarisation dynamics is determined by the heat redistribution inside the AE and the depolarisation pattern almost does not depend on the intensity of heat exchange with the environmental medium. Indeed, comparing Figs 2a and 2c, one can easily see that, up to the 20th second, the time dependences of depolarisation are almost the same.

As follows from (7), beginning from the instant $t_0 \approx c_T \rho R^2 / 5.76\kappa = 50$ s, the temperature distribution inside the AE corresponds to the first spatial harmonic, i.e. series (6) contains only the first term. From this point on, temperature changes due to the heat flow to the environmental medium.

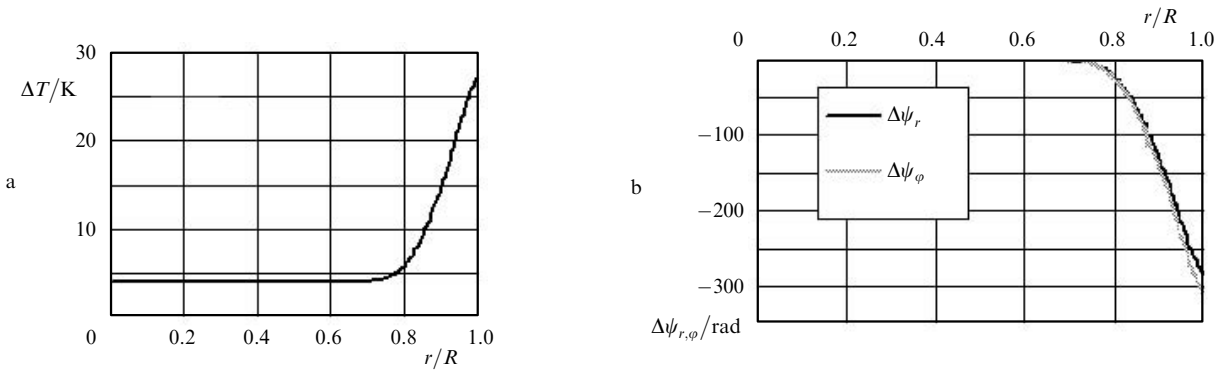

Figure 4. Radial dependences of temperature (a) and phase incursion (b) in an AE 15 mm in diameter one second after a pump pulse. ΔT is the difference between the temperature inside the AE and the temperature of surrounding air.

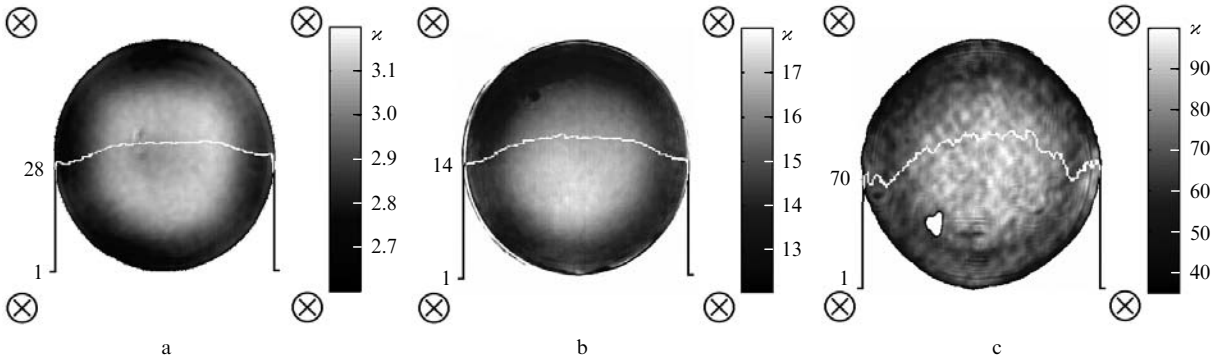

Figure 5. Small-signal gain $\varkappa$ in an AE 15 mm in diameter at the pump energy of 2.4 (a), 5.4 (b), and 13 kJ (c). The lines show the gain distribution in cross sections perpendicular to the plane of the figure. The positions of lamps are shown by crosses.

Hence, the depolarisation at this stage depends only on the intensity of heat exchange with this medium. The characteristic relaxation time of the integral depolarisation is twice as low as the temperature relaxation time, which follows from (5) when expanding $\Gamma(r)$ in the Taylor sine series to the first term and substituting (3) and (6).

As can be seen from Fig. 2b, in the case of natural cooling, the depolarisation due to the first spatial harmonic of temperature is extremely weak, because the heat flow at convective heat exchange is insignificant and, hence, the temperature gradient in the near-surface region is also small. The air cooling increases the heat flow from the AE and thus considerably worsens the situation. As a result, the depolarisation curve has one more maximum (at $t = 90$ s, Fig. 2b). However, the situation is reversed for a train of pump pulses (Fig. 3) and, hence, the advantage (natural cooling) turns into a disadvantage. The continuous increase in the AE temperature during this train results in the laser operation regime with a high steady-state depolarisation. For a train of pump pulses with a period of 5 min, this depolarisation is $\sim 8\,\%$ without air cooling (Fig. 3b) and 4 % for cooling by air flow (Fig. 3a).

Note that, at a particular time instant after the pump pulse, the depolarisation is smaller that its steady-state value. This occurs because the temperature gradient before the pump pulse is directed to the AE centre and the new pump pulse heats mainly the peripheral region of the AE (Fig. 4a). Thus, after the pump pulse, the temperature inside the AE is at first equalised and the depolarisation considerably decreases; then, the temperature gradient is again directed to the AE centre and the depolarisation increases. In principle, this can be used to reduce the depolarisation using a prior 'idle' pump pulse. In addition, to decrease the depolarisation at the pump pulse instant, one can switch off the air cooling of the AE, for example, one minute before the pump pulse. This method combines two advantages: intense heat removal to the environmental medium and a low temperature gradient immediately before the pump pulse.

Another method to reduce the depolarisation is to block the UV portion of the pump lamp radiation, which does not participate in the formation of inverse population. This can be done either by using a light filter surrounding the AE or by adding an UV-absorbing substance into the liquid around the AE. Usually, one uses potassium dichromate $K_2Cr_2O_7$.

5. Conclusions

A method for determining the temperature distribution and thermally induced phase distortions in rod laser amplifiers from the measured transverse distribution of the depolarisation degree is proposed and realised experimentally. The method demonstrates excellent coincidence of theory and experiment even at a strong radial inhomogeneity of the heat release.

Using this method, we have experimentally studied the dynamics of thermal effects in an amplifier based on a neodymium glass rod 15 mm in diameter in the case of natural or forced-air cooling. The experiments have been performed both with a single pump pulse and with a train of pump pulses with a period of 5 min.

It is shown that the depolarisation degree near the rod side surface reaches unity. In the case of a single pulse, air cooling is unfavourable because the temperature gradient in this case is high and, hence, the depolarisation lasts much longer than in the case of natural cooling. At the same time, in the case of a pulse train, the average temperature in the glass rod increases thus increasing the residual depolarisation before each new pulse. The air cooling threefold decreases the residual polarisation relaxation time and, hence, increases the maximum allowable pulse repetition rate.

The proposed method can be useful not only for determining the maximum allowable pulse repetition rate of laser amplifiers, but also for the express control of their condition immediately before the pump pulse.

References

1. Pennington D.M., Perry M.D., Stuart B.C., Boyd R.D., Britten J.A., Brown C.G., Herman S.M., Miller J.L., Nguyen H.T., Shore B.W., Tietbohl G.L., Yanovsky V. *Proc. SPIE Int. Soc. Opt. Eng.*, **3047**, 490 (1997).
2. Waxer L.J., Maywar D.N., Kelly J.H., Kessler T.J., Kruschwitz B.E., Loucks S.J., McCrory R.L., Meyerhofer D.D., Morse S.F.B., Stoeckl C., Zuegel J.D. *Optics & Photonics News*, **16**, 30 (2005).
3. Kitagawa Y., Fujita H., Kodama R., Yoshida H., Matsuo S., Jitsuno T., Kawasaki T., Kitamura H., Kanabe T., Sakabe S., Shigemori K., Miyanaga N., Izawa Y. *IEEE J. Quantum Electron.*, **40**, 281 (2004).
4. Danson C.N., Brummitt P.A., Clarke R.J., Collier J.L., Fell B., Frackiewicz A.J., Hancock S., Hawkes S., Hernandez-Gomez C., Holligan P., Hutchinson M.H.R., Kidd A., Lester W.J., Musgrave I.O., Neely D., Neville D.R., Norreys P.A.,

Pepler D.A., Reason C.J., Shaikh W., Winstone T.B., Wyatt R.W.W., Wyborn B.E. *Nuclear Fusion*, **44**, S239 (2004).
5. Gaul E., Martinez M., Ditmire T., Barber P., Blakeney J., Douglas S., Hammond D., Henderson W., Ringuette M. *Proc. Adv. Solid-State Photonics* (Nara, Japan, 2008) p. MC3.
6. Collier J.L., Chekhlov O., Clarke R.J., Divall E.J., Ertel K., Fell B.D., Foster P.S., Hancock S.J., Hooker C.J., Langley A., Martin B., Neely D., Smith J., Wyborn B.E. *Proc. Conf. on Lasers and Electro-Optics* (Baltimore, MD, 2005) p. JFB1.
7. Aoyama M., Yamakawa K., Akahane Y., Ma J., Inoue N., Ueda H., Kiriyama H. *Opt. Lett.*, **28**, 1594 (2003).
8. Liang X., Leng Y., Wang C., Li C., Lin L., Zhao B., Jiang Y., Lu X., Hu M., Zhang C., Lu H., Yin D., Jiang Y., Lu X., Wei H., Zhu J., Li R., Xu Z. *Opt. Express*, **15**, 15335 (2007).
9. Yanovsky V., Chvykov V., Kalinchenko G., Rousseau P., Planchon T., Matsuoka T., Maksimchuk A., Nees J., Cheriaux G., Mourou G., Krushelnick K. *Opt. Express*, **16**, 2109 (2008).
10. Lozhkarev V.V., Freidman G.I., Ginzburg V.N., Katin E.V., Khazanov E.A., Kirsanov A.V., Luchinin G.A., Mal'shakov A.N., Martyanov M.A., Palashov O.V., Poteomkin A.K., Sergeev A.M., Shaykin A.A., Yakovlev I.V. *Laser Phys. Lett.*, **4**, 421 (2007).
11. Mezenov A.V., Soms L.N., Stepanov A.I. *Termooptica tverdotel'nykh laserov* (Thermooptics of Solid-state Lasers) (Moscow: Mashinostroenie, 1986).
12. Landau L.D., Lifshits E.M. *Theory of Elasticity* (Oxford, Pergamon Press, 1970; Moscow: Nauka, 2004).
13. Nye J.F. *Physical Properties of Crystals: Their Representation by Tensors and Matrices* (Oxford: Clarendon Press, 1957; Moscow: Inostrannaya Literatura, 1960).
14. Korn G.A., Korn T.M. *Mathematical Handbook for Scientists and Engineers* (New York: McGraw-Hill, 1968; Moscow: Nauka, 1984).